Available online at www.sciencedirect.com

SCIENCE DIRECT®

Ore Geology Reviews 29 (2006) 77–94

ORE GEOLOGY REVIEWS

www.elsevier.com/locate/oregeorev

Geological characteristics and genesis of the Tuwu porphyry copper deposit, Hami, Xinjiang, Central Asia

Chunming Han [a,*], Wenjiao Xiao [a], Guochun Zhao [b], Jingwen Mao [c], Jianmin Yang [c], Zhiliang Wang [c], Zhen Yan [a], Qigui Mao [a]

[a] *People's Republic of China State Key Laboratory of Lithosphere Tectonic Evolution, Institute of Geology and Geophysics, Chinese Academy of Sciences, Beijing 100029, People's Republic of China*

[b] *Department of Earth Sciences, The University of Hong Kong, Pokfulam Road, Hong Kong, China*

[c] *Institute of Mineral Deposits, Chinese Academy of Geological Sciences, 26 Baiwanzhuang Road, Beijing, 100037, People's Republic of China*

Received 4 January 2005; accepted 24 July 2005
Available online 14 November 2005

Abstract

The Tuwu copper deposit, located in the Dananhu–Tousuquan island arc between the Kazakhstan–Junggar and Tarim plates, is one of the largest porphyry copper deposits in western China. Ore-hosting rocks consist of Early Carboniferous (333 ± 2 Ma) granodiorite- and plagiogranite-porphyries. Both the porphyries are elongate. The orebodies, consisting of veinlet-disseminated mineralization within the porphyries, grade range from 0.30% to 1.50% Cu. Mineralization can be assigned to six stages. Wall-rock alteration associated with the mineralization include silicification, chloritization, epidotization, sericitization and carbonatization. Three alteration zones have been recognized: phyllic zone, chlorite–biotite zone and propylitic zone. Re–Os dating indicates a 322.7 ± 3 Ma age for the deposit. $\delta^{34}S$ values of the ore sulfides range from $-0.9‰$ to $+1.3‰$, with a mean of 0.11‰, reflecting a deep sulfur source. $\delta^{18}O$ values of quartz in the ores range from 7.70‰ to 9.70‰, and the $\delta^{18}O$ value of chlorite in the ores is 6.62‰. Calculated $\delta^{18}O_{water}$ values of quartz and chlorite range from $-5.37‰$ to $+6.62‰$ and the δD values range from $-48‰$ to $-63‰$, suggesting that the ore fluids were mainly magma-derived in the early stage of mineralization. However, values for the late mineralization stage decrease, suggesting the addition of meteoric waters during the mineralization. Fluid inclusions within quartz grains are generally 3 to 30 μm in size, with gas proportions ranging from 5% to 60%, mostly from 10% to 15%. Homogenization temperatures of fluid inclusions are relatively low, bracketed between 101 and 409 °C, mostly between 100 and 200 °C. Salinities exhibit a wide range from 0.35 to 14.61 wt.% NaCl equiv., with a mean of 7.72 wt.% NaCl equiv., suggesting that ore fluids have low to moderate salinity. The ore-bearing plagiogranite porphyries show a strong depletion in heavy rare-earth elements, with average values of Yb and Y of 0.65 and 5.90 ppm, respectively, this being a characteristic geochemical signature for adakite. The geochemical signature of the

* Corresponding author. Tel.: +86 10 6200 7917; fax: +86 10 6201 0846.
E-mail address: CM-Han@mail.igcas.ac.cn (C. Han).

0169-1368/$ - see front matter
doi:10.1016/j.oregeorev.2005.07.032

adakites within the granitoid rocks represents a characteristic guide for further exploration for copper porphyry-type ore deposit in Eastern Tianshan.

Keywords: Porphyry copper deposit; Ore fluid; Fluid inclusions; Hydrothermal alteration; Radiometric age; Tuwu, Xinjiang, China

1. Introduction

The Chinese East Tianshan is the easternmost segment of the Tianshan Mountain Range in the southern Altaids (Xiao et al., 2004). The East Tianshan polymetallic belt is one of the important producers of Cu–Au–Ni–Fe–Ag in China. The porphyry Cu deposits relate to the late evolutionary stages of a subduction-related oceanic or continental, marginal arc (Mao et al., 2005; Fig. 1). The province also contains post-collisional metallic mineral deposits formed between 290 and 240 Ma. These are the products of large-scale emplacement and eruption of magmas possibly caused by lithosphere delamination and rifting within the East Tianshan (Xia et al., 2004).

Tuwu is the largest, and economically most important, deposit in the East Tianshan belt with total Cu metal reserves of 2.04 Mt. It was discovered in 1997 and exploited during the period 1998–2002; construction of the now-operating mine began in 2003. Since the discovery of the deposit, many scientific studies have been conducted that have addressed the geology and geochemistry of the Cu ores (Qin, 2000; Liu et al., 2001; Qin et al., 2001, 2002; Rui et al., 2001; Wang et al., 2001; Chen and Qu, 2002; Han, 2002; Han and Zhao, 2003; Han et al., 2003), radiogenic isotope dating and stable studies (Qin, 2000; Rui et al., 2001, 2002a; Han, 2002; Han and Zhao, 2003; Liu et al., 2003; Han et al., 2003), and the ore-forming environment (Qin, 2000; Qin et al., 2001; Han, 2002; Li et al., 2002; Rui et al., 2002b; Qin et al., 2003; Han and Zhao, 2003; Han et al., 2003; Liu et al., 2003; Xiao et al., 2004; Zhang et al., 2004a,b). However, most of the documentation of Tuwu deposit has been reported in the Chinese literature; the international geological community knows little about this deposit until now.

This paper introduces the Tuwu discovery to the international community and summarizes petrographic, stable isotope, and fluid inclusion data from the Cu ores in the deposit, as well as comparing Tuwu with other porphyry Cu deposits in China. Although Tuwu is one of the largest and economically important of the Paleozoic Cu deposits along the margins of Tarim

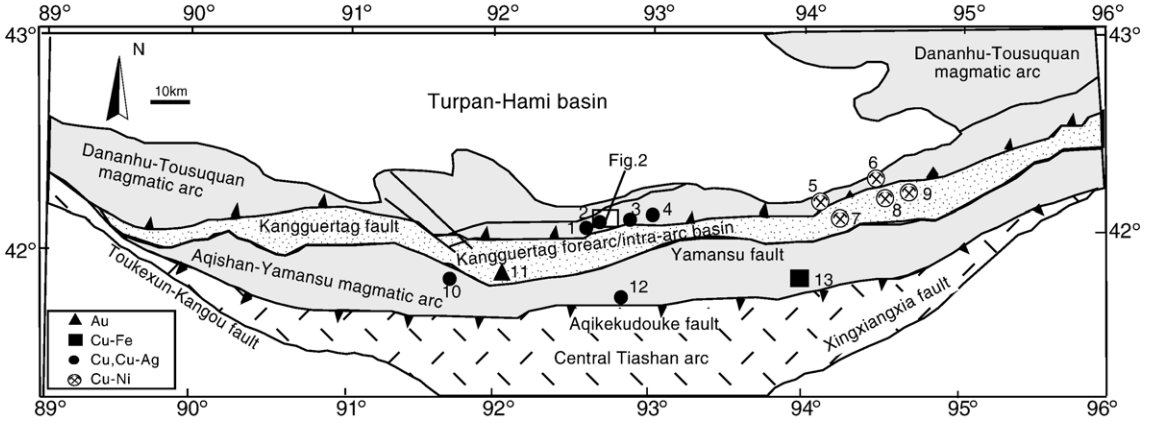

Fig. 1. Distribution of tectonic units and porphyry copper deposits in East Tianshan (after Han and Zhao, 2003). Deposits: 1 — Yandong porphyry Cu; 2 — Tuwu porphyry Cu; 3 — Linglong porphyry Cu; 4 — Chihu porphyry Cu; 5 — Tudun Cu–Ni; 6 — Xiangshan Cu–Ni; 7 — Erhongwa Cu–Ni; 8 — Huangshan Cu–Ni; 9 — Huangshandong Cu–Ni; 10 — Weiquan Cu–Ag skarn; 11 — Jiabaishan orogenic Au; 12 — Lubaishan volcanic Cu; 13 — Yanmasu volcanic Cu–Fe.

Craton, and in all of China for that matter, it remains poorly understood genetically. The data from the Tuwu deposit provide important new constraints on conditions of ore formation, both in the deposit itself, and by inference, throughout much of Central Asia.

2. Regional geological setting

The East Tianshan province (Fig. 1) contains a number of Paleozoic terranes that amalgamated between the Siberian and Tarim cratons, and underwent complex tectonic evolution (Coleman, 1989; Xiao et al., 1990; Windley et al., 1990; Allen et al., 1992; Sengör et al., 1993, 1996; He et al., 1994; Yang, 1996; Ma et al., 1997; Yang et al., 1997, 1998; Gao et al., 1998; Zhou et al., 2001, 2004; Qin et al., 2002, 2003; Mao et al., 2002, 2003, 2005; Xiao et al., 2004; Zhang et al., 2004a). The province is divided into three tectonic zones (North, Central and South Zones), which are separated by the regional-scale Kangguer and Yamansu deep faults. The North Zone, situated north of the Kangguer fault, is also called the Dananhu–Tousuquan island-arc, and contains several porphyry Cu deposits of different sizes, including the Yandong, Tuwu, Linglong and Chihu deposits (Fig. 1). The Central Zone lies between the Kangguer and Yamansu faults, an area in which most rocks have undergone greenschist facies metamorphism and ductile deformation, and where there are a number of important orogenic Au deposits (e.g., Jiabaishan) and magmatic Cu–Ni sulfide deposits (e.g., Huangshan and Huangshan East). The South Zone is also called the Aqishan–Yamansu rift zone, and is located between the Yamansu and Aqikekudouke faults. It hosts numerous Fe, Cu, Au and Ag ore deposits. Representative among these are the Yamansu volcanic Cu–Fe deposit, the Weiquan Cu–Ag skarn deposit and the Lubaishan volcanic Cu deposit (Fig. 1).

The North Zone of the East Tianshan region, which hosts the Tuwu porphyry Cu deposit, is located south of the Turpan–Hami basin and north of the Kangguer fault. The structures of the zone are dominated by a series of NW- and NE-trending strike-slip faults. The strata consist principally of Devonian–Carboniferous calc-alkaline volcanic and pyroclastic rocks, Permian calc-alkaline volcanic, pyroclastic and clastic rocks, and Jurassic terrestrial clastic rocks interleaved with coal seams. Permian and older strata have been regionally metamorphosed at lower greenschist and prehnite–pumpellyite facies. Intrusive rocks are chiefly middle Variscan mafic and ultramafic rocks, quartz diorites, plagiogranites, monzogranites and granites. Plagiogranite porphyry occurs in association with the porphyry Cu deposits at Yandong, Tuwu, Linglong and Chihu (Fig. 1).

3. Geology of the Tuwu region

3.1. Local stratigraphy

The Tuwu porphyry Cu deposit is hosted in the Carboniferous Qi'eshan Group of the Dananhu–Tousuquan island arc, which consists predominantly of basalt, andesite, spilite, keratophyre, andesitic brecciated lavas, lithic sandstone, pebbly lithic sandstone, polymictic conglomerate and tuffaceous sedimentary rocks. The strata of the Tuwu region, generally with well-developed schistosity, striking close to E–W and dipping to the south at 43° to 63°, can be divided into the following six units of the Qi'eshan Group, from the lowermost upwards (Fig. 2).

Unit 1 is located in the NE part of the map area (Fig. 2) and is composed of medium- and coarse-grained schistose greywackes. The unit strikes WNW–ESE and dips 44° to the south, with a maximum apparent outcrop thickness of >100 m. To the north, unit 1 is covered by the rocks of the Jurassic Xishanyao Formation and Quaternary sediments.

Unit 2, consisting of volcanic breccias, is found in the NE part of the ore district, with a maximum apparent thickness of about 100 m. The unit strikes nearly E–W and is covered by the Jurassic Xishanyao Formation and Quaternary sediments. In the eastern part, it is intruded by a diorite porphyry stock. The breccias are composed of purplish-red andesite and grayish-green tuffs; the andesitic fragments are mostly angular in shape, with a diameter of 3 to 20 mm, and the tuffaceous fragments are also angular, but with a diameter of only 3 to 8 mm.

Unit 3 lies in the northern part of the Tuwu region, extending in a nearly E–W direction and dipping south, and consists of amygdaloidal basalts. The NE part of the unit is in contact with volcanic breccias, and the NW part is covered by sedimentary rocks of the

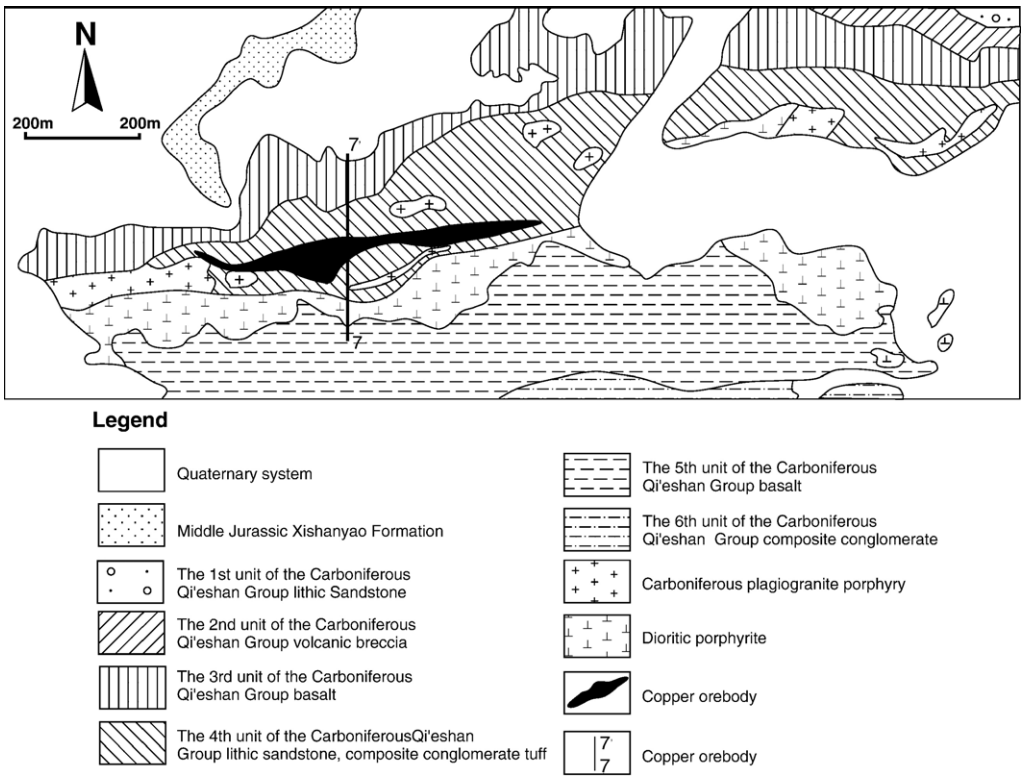

Fig. 2. Geological map of the Tuwu porphyry copper deposit (after Wang et al., 2001).

Jurassic Xishanyao Formation and Quaternary sediments. The unit is about 130 m thick, and shows well-developed schistosity and amygdaloidal structures; locally, the amygdales are flattened and stretched.

Unit 4 consists of pebbly lithic sandstone, which locally grades into polymictic conglomerate, lithic sandstone and tuffaceous sediments that are intercalated with basalt, andesite and dacite flows. The strata strike ENE–WSW and dip SE at 45–60°. The unit is best exposed in the central part of the Tuwu region, where it reaches a maximum outcrop thickness of 170 m and is dominated by pebbly lithic sandstones. The rocks of the unit have been strongly altered and the original textures and structures of the protoliths are only locally preserved.

Unit 5 is composed of amygdaloidal spilite-keratophyres intercalated with brecciated andesite flows, which are mostly exposed in the southern part of the region, with an outcrop thickness of almost 200 m. These rocks host the mineralized intrusion of the Tuwu deposit.

Unit 6 consists of grayish-green polymictic conglomerate, locally intercalated with lenticular fine-grained lithic sandstone. Distributed in the southern part of the Tuwu region, the unit strikes E–W and dips south at 63°, with an average thickness of about 25 m. Pebbles in the conglomerate are sub-rounded and are composed of granite, basalt and felsic porphyry.

3.2. Intrusive rocks

Ore-bearing plagiogranite porphyries were emplaced into across the region as 23 intrusive stocks and plugs, the largest of which occupies a surface outcrop of ~0.03 km^2. Viewed in surface outcrop, the intrusions are mostly irregular in shape, but viewed in vertical section, the intrusions occur as apophyses of a larger body. The rocks have porphyritic textures and massive structures. Phenocrysts minerals are quartz, plagioclase and biotite; the matrix exhibits a subhedral texture. Hydrothermal alteration is marked by silicification, sericitization, carbonatization, chloritization

Table 1
Representative major and trace element analysis of the altered plagiogranite porphyry in the Tuwu deposit

Sample	TW28[c]	TW208[d]	TW203[d]	TW205-1 [d]	Btw38[e]	Btw92[e]	T-4[f]	T-71[f]	R-1[g]	R-2[g]
Wt.%										
SiO_2	70.65	68.21	70.32	80.73	64.34	71.83	65.32	69.35	72.28	67.50
TiO_2	0.28	0.37	0.26	0.19	0.47	0.10	0.26	0.71	0.21	0.24
Al_2O_3	15.57	17.08	16.15	12.03	17.71	14.77	15.43	15.66	12.32	14.80
Fe_2O_3	1.18	0.60	0.60	0.28	2.23	1.70	0.40	0.17	1.34	0.87
FeO	0.20	1.13	0.76	0.26	1.97	0.40	2.15	1.05	1.78	1.72
MnO	0.02	0.03	0.02	0.01	0.04	0.04	0.09	0.11	0.11	0.08
MgO	1.06	1.35	0.82	0.07	2.20	0.70	0.73	0.55	1.33	0.75
CaO	0.90	1.56	1.10	0.11	2.30	0.30	5.62	2.77	1.45	3.40
Na_2O	7.36	4.89	5.24	2.73	4.60	5.20	1.74	4.15	3.42	4.21
K_2O	0.94	2.00	2.05	2.14	1.93	1.32	1.39	2.11	1.91	0.97
P_2O_5	0.11	0.12	0.08	0.06	0.20	0.09	0.13	0.13	0.11	0.12
A/NCK[a]	1.05	1.31	1.26	1.72	1.28	1.40	1.06	1.11	1.19	1.05
Mg#[b]	72.1	63.2	58.7	24.4	56.9	51.7	35.8	46.5	49.9	38.8
LOI	2.04	2.52	2.47	1.43	1.56	2.80	6.37	3.22	2.00	5.06
$\sum$	100.31	99.86	99.87	100.04	99.55	99.25	99.63	99.98	98.26	99.72
ppm										
La	8.91	11.4	7.38	7.71	10.3	12.70	8.55	14.46	5.17	8.79
Ce	16.53	23.5	15.1	15.5	18.6	22.50	17.69	22.84	10.52	16.71
Pr	2.56	2.78	1.79	1.83			2.36	2.69	1.04	1.97
Nd	10.84	11.0	6.83	7.19	10.10	9.73	9.61	9.35	4.19	9.21
Sm	1.59	1.93	1.21	1.27	2.30	1.75	1.76	1.78	0.85	1.34
Eu	0.66	0.808	0.594	0.60	0.75	0.56	0.47	0.52	0.38	0.62
Gd	1.29	1.60	1.05	1.19	1.96	1.75	1.34	1.47	0.86	1.54
Tb	0.3	0.199	0.13	0.143	0.28	0.29	0.20	0.22	0.13	0.25
Dy	0.98	1.11	0.833	0.924			1.12	1.26	0.70	1.19
Ho	0.2	0.211	0.149	0.179			0.23	0.25	0.14	0.23
Er	0.58	0.59	0.44	0.51			0.67	0.74	0.38	0.75
Tm	0.1	0.08	0.06	0.07			0.11	0.12	0.06	0.10
Yb	0.65	0.59	0.41	0.58	0.84	0.87	0.72	0.79	0.38	0.67
Lu	0.1	0.08	0.05	0.07	0.14	0.15	0.12	0.13	0.07	0.11
$\sum$REE	45.29	55.88	36.03	37.77	45.27	50.30	44.95	56.62	24.87	43.48
δEu	1.38	1.38	1.59	1.48	1.06	0.98	0.91	0.96	1.36	1.33
$(La/Yb)_N$	9.03	12.73	11.86	8.76	8.08	9.62	7.82	12.06	8.96	8.64
Cr	6.2	15.7	15.7	16.6						
Ni	12	2.7	2.63	6.8						
Co	3.7	6.06	3.00	4.94						
Rb	5.2	46.6	35	21.8	28.1	16.1				
Ba	109	1483	850	586	394	341				
Sr	279	619	347	714	405	226				
Ta	0.7	0.321	0.441	0.117	0.185	0.263				
Nb	3.2	3.15	2.72	2.21	2.70	3.90				
Hf	3.3	1.23	0.588	1.09	1.75	2.55				
Zr	156	41.9	15.6	37	100	69.9				
Cs	0.5	3.57	2.43	1.21						
Y	4.96	6.17	4.42	5.23	7.90	6.70				
Th	1.1	1.60	1.428	1.226	0.75	1.47				
U	0.3	0.41	0.191	0.205						
Sr/Y	56.25	100.32	78.51	136.52	51.27	33.73				
Y/Yb	7.63	10.46	10.78	9.02	9.40	7.70				

[a] $A/NCK = Al_2O_3/(CaO+Na_2O+K_2O)$ molar ratio; [b] $Mg\# = 100 * [MgO/(MgO+FeO+Fe_2O_3)]$ molar ratio.
Data sources: c — this study, d — Zhang et al. (2004b), e — Li et al. (2002), f — Chen and Qu (2002), g — Rui et al. (2002a).

and kaolinitization. Quartz phenocrysts in the fresh plagiogranite have resorption borders. The quartz phenocrysts fall into two size fractions: the larger ones (2 to 4 mm in diameter) make up ~5% of the intrusions and the smaller ones (0.2 to 0.5 mm) generally make up ~10%.

The late-stage is represented by strong silicification, sericitization and jarositization, which converted plagiogranite-porphyry to albite–granite-porphyry, in which albite constitutes 50% to 55%, quartz 10% to 20% and sericite ~15% of the rock, with minor amounts of calcite (<10%). Accessory minerals are zircon, magnetite, apatite and rutile.

Major element compositions of the plagiogranite-porphyry are characterized by the following chemistry (wt.%): 64.34 to 80.73 SiO_2, 12.03 to 17.71 Al_2O_3, 0.07 to 2.20 MgO, 1.16 to 2.51 FeO_{total}, 1.74 to 7.36 Na_2O and 0.68 to 2.11 K_2O (Table 1). The plagiogranite-porphyry, host to mineralization, is cut by numerous quartz-sulfide and biotite–chlorite-sulfide veinlets, and locally by carbonate, anhydrite and minor sulfide veinlets. Biotite contains high MgO contents, with Mg/(Mg+Fe+Mn) ratios of 0.35 to 0.60 (Rui et al., 2001), probably produced under high-fO_2 conditions; an interpretation further supported by the presence of large amounts of hematite and magnetite in the ores. The total REE abundance of the plagiogranite-porphyry rocks ranges from 45 to 75 ppm (Table 1). Chondrite-normalized rare earth element (REE) patterns are strongly fractionated, with LREE enrichment and HREE depletion (Yb: 0.38 to 0.87 ppm). REE patterns display steep negative slopes without Eu anomalies (Fig. 3a,b). All the plagiogranite porphyry rocks show similar MORB-normalized trace element patterns, with depletion in Nb and Y (Fig. 3c), similar to those of most modern subduction-related volcanic and plutonic rocks (Wood et al., 1979; Briqueu et al., 1984; Gu et al., 2003). The low Nb depletion is typical of calc-alkaline magmatic rocks formed in subduction-zone environments and may be regarded as an indicator of crustal involvement in magmatic processes (Rollinson, 1993; Lan et al., 1996).

The diorite porphyry body strikes close to E–W and occupies a surface area of ~0.19 km^2. It has a porphyritic texture and a massive structure. Phenocryst minerals are anorthite and biotite, and the matrix contains anorthite, biotite, hornblende and quartz and displays a subhedral texture. Accessory minerals are

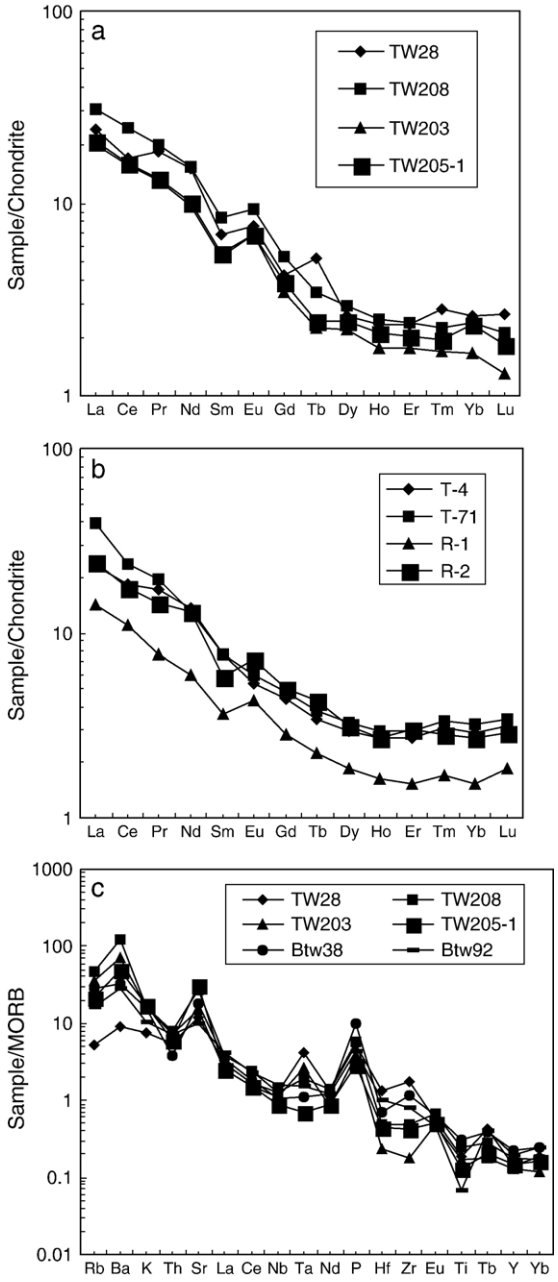

Fig. 3. (a and b) Chondrite-normalized REE diagrams and (c) MORB-normalized trace-element diagrams for the altered porphyries at the Tuwu deposit.

magnetite, apatite and zircon. Types of wall-rock alteration include chloritization, sericitization, epidotization, silicification and carbonatization. Intrusive contacts between the diorite porphyrite and the

Table 2
Representative major and trace element analysis of the diorite porphyrite in the Tuwu deposit

Sample	ZK004-74[a]	ZK004-76[a]	ZK004-35[a]	ZK004-59[a]	ZK004-55[a]	TW42[a]	TW1[a]	ZK004-66[a]	T-1[b]	Y-1[b]	T-9[b]
55[a]											
SiO_2	48.07	50.79	53.96	54.09	55.52	50.26	47.55	58.16	57.18	52.95	49.52
TiO_2	0.96	0.97	1.08	1.00	0.96	1.02	0.93	0.98	0.86	1.06	0.93
Al_2O_3	19.28	17.98	18.34	17.97	17.48	19.00	19.01	20.78	16.92	17.37	19.38
Fe_2O_3	2.14	1.82	2.17	1.97	2.74	4.54	1.99	1.62	5.15	4.60	0.46
FeO	5.89	5.59	6.25	5.80	6.02	6.13	5.76	2.60	2.19	3.52	8.27
MnO	0.05	0.07	0.07	0.07	0.06	0.07	0.06	0.03	0.12	0.14	0.07
MgO	4.62	6.10	6.34	6.21	5.86	5.32	4.46	2.81	3.65	5.67	6.76
CaO	3.61	5.77	3.00	3.59	2.80	4.33	3.46	2.96	7.74	6.15	5.64
Na_2O	4.39	3.20	2.74	2.57	2.40	2.82	4.30	3.28	3.87	3.16	2.56
K_2O	2.41	0.15	0.66	0.08	0.24	0.06	2.47	2.68	0.13	2.73	0.10
P_2O_5	0.16	0.24	0.26	0.22	0.26	0.26	0.18	0.22	0.20	0.38	0.20
CO_2	2.92	2.21	0.19	0.85	0.38	0.58	4.06	1.06	0.01	0.29	0.90
SO_3	0.91		0.28	0.34	1.02		0.06				
H_2O^+	4.46	4.64	4.98	4.96	5.04	4.92	5.30	3.50	2.46	2.76	4.89
Σ	100.13	99.53	100.32	99.86	100.99	99.31	99.97	100.68	100.48	100.78	99.68
ppm											
La	7.31	7.59	6.42	7.40	5.81	7.99	7.83	26.62	13.14	19.16	9.94
Ce	14.70	16.92	14.78	17.03	14.21	18.19	17.26	62.79	27.45	42.54	17.87
Pr	2.27	2.66	2.42	2.51	2.11	3.07	2.48	7.07	3.55	5.38	2.45
Nd	10.43	12.73	9.96	12.79	10.85	13.85	13.83	31.95	17.46	23.95	10.69
Sm	2.75	3.39	2.49	3.28	2.34	3.52	3.19	6.36	3.91	5.03	2.43
Eu	0.92	1.16	0.91	0.98	0.81	1.06	1.13	1.19	1.30	1.55	0.80
Gd	3.00	3.56	3.16	3.39	2.59	3.46	3.59	5.18	3.54	4.43	2.36
Tb	0.50	0.60	0.50	0.52	0.40	0.61	0.57	0.81	0.62	0.69	0.37
Dy	2.89	3.28	2.99	2.95	2.34	3.45	2.99	4.13	3.41	3.64	2.36
Ho	0.58	0.64	0.62	0.60	0.48	0.71	0.58	0.82	0.70	0.74	0.48
Er	1.45	1.60	1.51	1.58	1.15	1.72	1.54	2.17	1.74	1.96	1.43
Tm	0.21	0.23	0.23	0.22	0.17	0.25	0.22	0.33	0.25	0.27	0.22
Yb	1.41	1.46	1.49	1.49	1.23	1.61	1.51	2.11	1.63	1.74	1.39
Lu	0.23	0.24	0.25	0.24	0.20	0.27	0.24	0.35	0.27	0.29	0.22
∑REE	48.85	55.93	47.73	54.98	44.42	59.80	56.96	151.88	78.97	111.37	66.51
δEu	0.98	1.02	1.00	0.90	1.01	0.92	1.03	0.62	1.06	0.99	1.02
$(La/Yb)_N$	3.35	3.36	2.79	3.21	3.06	3.21	3.36	6.68	5.31	6.67	4.63
Cr	195	139	138	151	154						
Ni	85	98	89	97	99						
Co	23	21	18	20	27						
Rb	21	4.3	17	7.7	6.2						
Ba	81	81	98	98	83						
Sr	315	496	467	462	495						
Ta	4.3	2.90	4.30	2.10	1.50						
Nb	4.1	3.3	3.9	3.60	3.50						
Hf	3.3	2.90	3.30	2.90	2.90						
Zr	159	106	126	123	104						
Cs	3.10	0.90	1.30	1.10	0.90						
Y	15.57	13.94	13.20	14.06	11.44	14.87	13.99				
Th	1.40	1.40	4.80	2.50	1.80						
U	0.4	0.4	0.4	0.5	0.5						
Sr/Y	20.23	35.58	35.38	32.86	43.27						
Y/Yb	11.04	9.55	8.86	9.44	9.30	9.24	9.26	8.78	7.02	9.60	

Data sources: a — this study, b — Chen and Qu (2002).

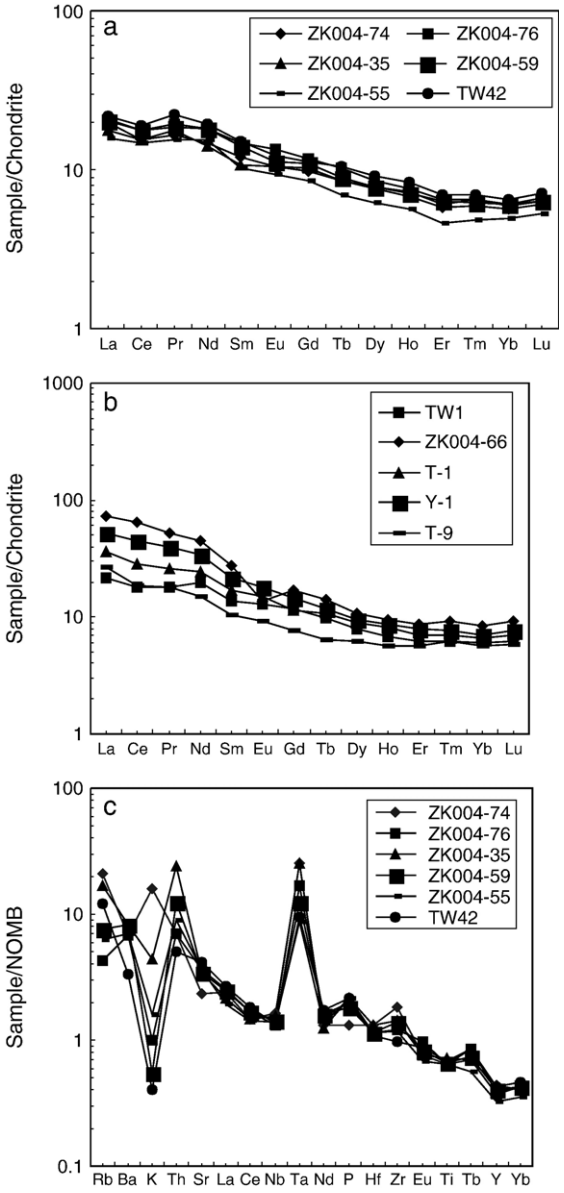

Fig. 4. (a and b) Chondrite-normalized REE diagrams and (c) MORB-normalized trace-element diagrams for the diorite porphyrite at the Tuwu deposit.

plaiogranite porphyry can be observed in the outcrop; the plaiogranite porphyry usually occurs as dykes in the former.

Major element chemistry of the diorite porphyrites is characterized by 47.55% to 58.16% SiO_2, 16.92% to 19.28% Al_2O_3, 2.81% to 6.76% MgO; 4.06% to 10.22% FeO_{total}, 2.40% to 4.39% Na_2O and 0.08% to 2.68% K_2O (Table 2). Chondrite-normalized REE patterns of the diorite porphyrites are characterized by HREE depletion, and small negative Eu-anomalies (average δEu is 0.97) (Fig. 4a,b). Relatively low Y and high Sr contents are also observed in these rocks (Table 2). The chemical features of the diorite porphyrites are HFSE depletion and LILE enrichment, negative Ba, Nb and Y anomalies in the MORB-normalized patterns (Fig. 4c), suggesting they originated in a suprasubduction zone setting (Luchitskaya et al., 2005).

4. Geology of the deposit

The Tuwu copper deposit consists of the Tuwu and Eastern Tuwu orebodies (Fig. 2), which are situated <200 m apart from one another.

4.1. Characteristics of the Tuwu orebody

The orebody occurs as a thick tabular or bedlike unit, with a maximum length up to 1400 m and a width of up to 125 m at the surface. There is no distinct boundary between orebody and country rocks. Using a nominal cut-off grade of 0.50% Cu to outline the orebody, it has a continuous length of 900 m and an average width of 25 m. The orebody has a thick lenticular surface morphology and is elongate in the E–W direction. The exploratory profile section reveals that the orebody has a wedge shape that expands downwards. The orebody dips gently in the south and steeply in the north (Fig. 5), with the hanging wall dipping south at 60° to 65° and the footwall dipping 65° to 80° to south. The orebody has a tendency to pitch toward east.

Using a cut-off grade of 0.20% Cu, the ore tonnage is calculated to be 292.0 Mt, with 1.445 Mt of contained copper. Using the higher 0.5% cut-off grade, the ore tonnage is calculated to be 14.5 Mt and the contained copper, 0.99 Mt. In addition, 19.4 t of gold and 419 t of silver may be recovered as by-products. The copper grade of the ores in the Tuwu orebody ranges up to 1.5%. Using the cut-off grade of 0.5%, the average grade is 0.72% Cu, 0.16 g/t Au and 2.97 g/t Ag.

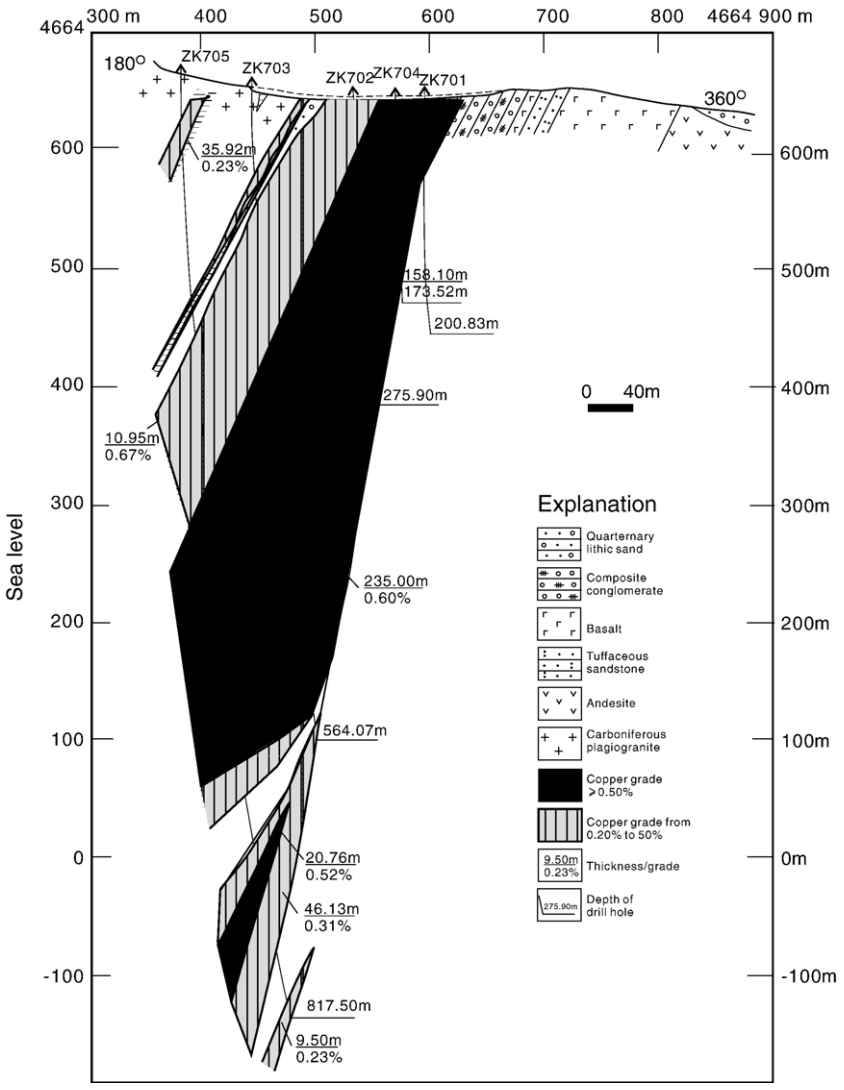

Fig. 5. Profile map of No. 7 prospect, Tuwu porphyry Cu deposit (scale 1:4000; after Wang et al., 2001).

4.2. Characteristics of the Eastern Tuwu orebody

In surface exposure, the Eastern Tuwu orebody is about 1300 m in length. The width of the orebody varies from east to west, (average 32 m, maximum 84 m) and is narrowest in the middle. It dips steeply to the south. Using a cut-off grade of 0.2% Cu, ore and metal reserves of the Eastern Tuwu orebody are calculated to be 178 Mt of ore grading 0.335% Cu, corresponding to 0.595 Mt of contained Cu. Using the 0.5% Cu cut-off grade, ore tonnage is 26.7 Mt at 0.582% Cu (0.155 Mt contained Cu). In addition, 18 t Au and 565 t Ag are expected to be recovered as by-products. The average grade of the mineralized body at surface is 0.30% Cu, and 0.35% Cu in ore encountered by drillholes; ore grade increases as the orebody thickens to the east.

4.3. Ore mineralogy

A variety of mineralization styles are present, include disseminated, veinlet-disseminated, veinlet-

like and less commonly nodular. The dominant ore minerals are chalcopyrite and pyrite, with lesser bornite, chalcocite, digenite, sphalerite, magnetite and rickardite. Gangue minerals include quartz, plagioclase, sericite, chlorite and biotite, with minor hornblende, pyroxene, epidote, zoisite and calcite. Malachite and limonite are, respectively, the main secondary carbonate and oxide ore minerals. Oxide minerals are anhedral, irregularly granular with a grain size typically ranging from 0.02 to 0.60 mm.

Chalcopyrite is the most important economic ore mineral in the Tuwu deposit, occurring in disseminated, veinlet-like and veinlet-disseminated ores. Bornite occurs in disseminated ores. Pyrite occurs in disseminated, veinlet-like and veinlet-disseminated ores. Pyrite from the Tuwu deposit contains significant amounts of trace elements, including as much as 200 ppm Ni and 3100 ppm Co. Sphalerite occurs in disseminated ores.

4.4. Stages of mineralization

Based on crosscutting relationships among minerals and mineral assemblages, mineralization in the Tuwu orebody can be divided into the following six mineralization stages (Fig. 6).

Stage 1 is characterized by Mg-rich biotite, accompanied by albite and K-feldspar — products of alkali-silicate metasomatism. Some metal sulfides also formed during this stage; chalcopyrite+bornite+pyrite is a representative ore mineral assemblage.

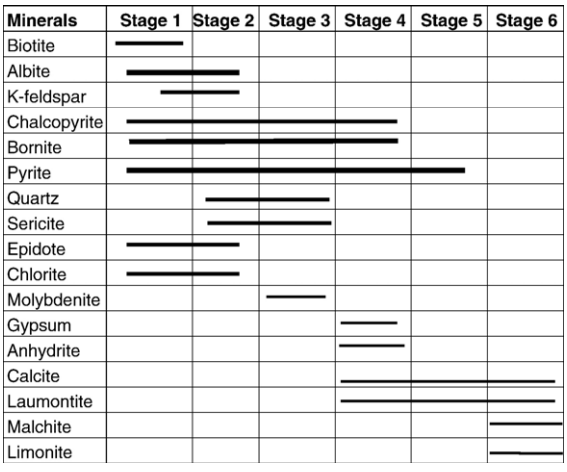

Fig. 6. Paragenetic sequence of minerals of the Tuwu deposit.

Stage 2 is characterized mainly by phyllic alteration, forming the quartz+pyrite+chalcopyrite assemblage that occurs as veins.

Stage 3 is represented by the formation of veins containing quartz+molybdenite.

Stage 4 is marked by the development of sulfates (gypsum+anhydrite), plus some sulfide veinlets.

Stage 5 is characterized by the presence of carbonate (calcite)+laumontite+minor sulfides.

Stage 6 is marked by supergene oxidation, resulting in the formation of some secondary minerals (e.g., malachite and limonite).

4.5. Wall-rock alteration

Wall-rock alteration related to mineralization in the Tuwu copper district includes silicification, chloritization, epidotization, sericitization and carbonatization. Wang et al. (2001) divided the altered rocks of the Tuwu deposit into 5 alteration zones: from the core zone outwards — quartz core zone, chlorite–biotite zone, phyllic zone, argillic zone and propylitic zone. The phyllic, chlorite–biotite and propylitic zones are most widespread and are thus described in detail here.

4.5.1. Phyllic zone

This zone consists dominantly of sericite and quartz, and sometimes contains small amounts of albite and chlorite. The principal altered primary rock is plagiogranite-porphyry, which occupies the central part of the alteration zones, where a strongly developed phyllic assemblage is often mistaken for a quartz core zone, but it is a quartz–sericite zone. In the strongly altered rock, sericite (muscovite and hydromuscovite) generally accounts for >30%. The phyllic zone hosts most Cu minerals and is the main site for most ore shoots.

4.5.2. Chlorite–biotite zone

In this zone, biotite usually occurs as spots and veinlets in association with pyrite and chalcopyrite. The altered primary rock is diorite-porphyrite, distributed on both sides of the phyllic zone. The chlorite–biotite zone is the main site of the orebodies. Biotite has a Mg/(Mg+Fe+Mn) ratio of 0.06, and is interpreted to have formed at relatively high oxygen

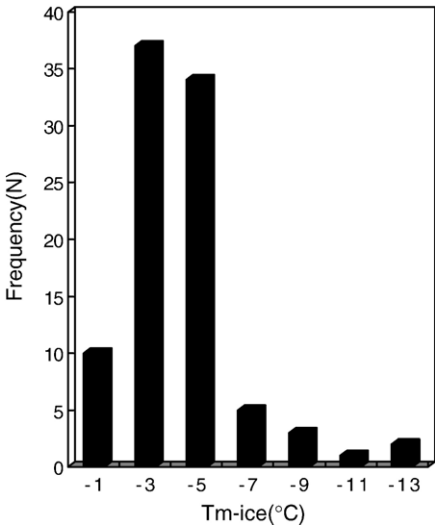

Fig. 7. Frequency distribution diagram of ice melting temperature for fluid inclusions in the Tuwu deposit.

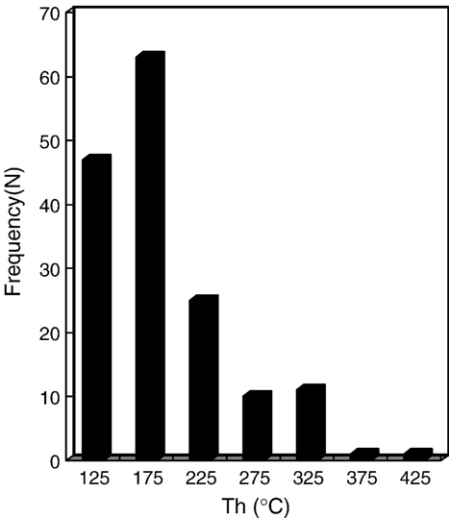

Fig. 9. Frequency distribution diagram of homogenization temperature for fluid inclusions in the Tuwu deposit.

fugacity ($fO_2 = 10^{-20}$ to 10^{-8}) in the process of magmatic-hydrothermal evolution (Rui et al., 2001). Minor K-feldspar has been found in this assemblage.

4.5.3. Propylitic zone

This zone is composed chiefly of chlorite, epidote and albite, and is the most widespread style of alteration. Minor Cu orebodies are hosted in this zone, but they are mainly low-grade. Chlorite alteration mainly occurs in ore-bearing trachybasalt, basaltic trachyandesite, trachyandesite, dacite and plagiogranite-porphyry, as well as barren dacite and rhyolite. Epidote is very common in this zone and occurs in both ore-bearing and barren propylites. Albite is another common altered mineral in the propylitic zone, though it is also found in other alteration zones, especially in Na_2O-rich host rocks.

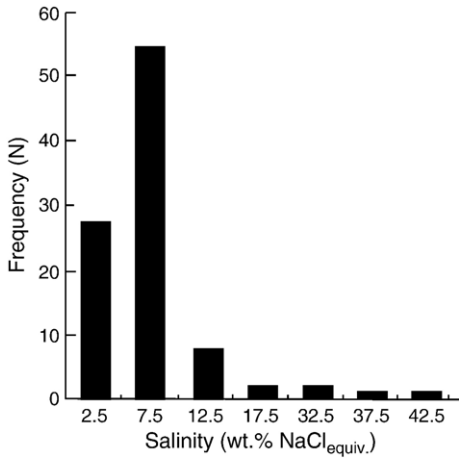

Fig. 8. Histograms of apparent salinity of fluid inclusions in equivalent wt.% NaCl.

5. Geochemical characteristics of the deposit

5.1. Fluid inclusions

Fluid inclusion studies have been carried out on doubly polished wafers of quartz grains from 13 samples using a Chaixmeca (−180~600 °C) heating–freezing stage equipped with a standard petrographic

Table 3
Oxygen isotopic compositions of quartz and chlorite

Specimen no.	Minerals	$\delta^{18}O_{Min}$ (‰)	δD_{H2O} (‰)	$\delta D_{F.I.}$	FT()	Reference
ZK705-521.7	Chlorite	8.00	6.62	−48	250	Rui
ZK4002-312	Quartz	7.70	−5.37	−63	180	Rui
ZK4002-333.33	Quartz	9.60	−2.11	−50	200	Rui
ZK705-452.5	Quartz	9.70	−2.01	−45	200	Rui
ZK705-521.7	Quartz	9.20	−2.51	−48	200	Rui

FT() = Formation temperature calculated from fluid inclusion data. Abbreviations: F.I. = fluid inclusion; Min = mineral.

Table 4
Carbon and oxygen isotopes of calcite

Specimen no.	Sample locality	Minerals	$\delta^{13}C_{PDB}$‰	$\delta^{18}O_{PDB}$‰	$\delta^{18}O_{SMOW}$‰
ZK002-149	ZK002, 149 m	Calcite	−6.2	−15.1	15.3
CK1502-444.5	ZK1502, 444.5 m	Calcite	−0.7	−24.0	6.1

microscope. In these quartz grains, fluid inclusions range in size from 3~30 μm. Gas volumes of the fluid inclusions are 5~60 vol.%; the majority are 10~15 vol.% gas.

Freezing experiments were performed before heating runs. Salinities were estimated based on ice-melting temperature ($T_{m\text{-}ice}$) in the system H_2O–NaCl, for dominantly aqueous inclusions. The ice melting data are between −0.2 and −12.4 °C (Fig. 7), corresponding to salinities of 0.35~16.4 wt.% NaCl equiv. (mode 7.5 wt.%; Fig. 8). Homogenization (to liquid) temperatures range between 101 and 409 °C, with temperatures around 175 °C being most common (Fig. 9).

5.2. Stable isotopes

Stable isotope studies were carried out in order to constrain the origin of the deposit. These included determinations of the O and H isotopic compositions of quartz and chlorite, C and O isotopic compositions for calcite, and S isotopic compositions for chalcopyrite and pyrite.

Oxygen and hydrogen isotopic compositions for five handpicked quartz and chlorite crystals from the Tuwu deposit are listed in Table 3. The measured $\delta^{18}O$ value is 7.70‰ to 9.70‰ for quartz and about 9.70‰ for chlorite. $\delta^{18}O_{H2O}$ values of the fluids are estimated between −5.37‰ and 6.62‰ using the quartz–water and chlorite–water fractionation equations and the temperature calculated from the fluid inclusion data. All the minerals separated for $\delta^{18}O$ analysis were also analyzed for hydrogen isotopic composition. δD values of fluid inclusion waters in quartz and chlorite fall into a range between −48‰ and −63‰. Taken together, these data indicate that both magmatic and meteoric waters were involved in the ore-forming processes.

Calcite, commonly observed as an interstitial mineral, is generally useful to provide information on the C and O isotopic compositions of the fluids present in the latest stage of copper mineralization. In this study, two calcite samples were analyzed for C and O isotopic compositions. As shown in Table 4, the analyzed calcite samples have distinctly different carbon and oxygen isotopic values. These late-stage calcites appear to have been mainly deposited by meteoric water.

Only a limited number of chalcopyrite and pyrite specimens were collected for S isotope analysis (Table 5). $\delta^{34}S$ values obtained range from −0.9‰ to 1.3‰, with a mean of +0.34‰, close to meteoritic values, suggesting a deep crust or upper mantle source for sulfur in the Tuwu deposit.

Table 5
Sulfur isotopes of chalcopyrite and pyrite

Specimen no.	Sample locality	Minerals	$\delta^{34}S$ (‰)
Ck1501-751.5	Zk1501, 751.5 m	Chalcopyrite	−0.90
Ck1501-687	Zk1501, 687 m	Chalcopyrite	−0.70
Ck1601-259	Zk1601, 259 m	Pyrite	1.30
Ck1601-261	Zk1601, 261 m	Pyrite	0.40
Ck1601-277	Zk1601, 277 m	Pyrite	0.70
Ck1601-291	Zk1601, 291 m	Pyrite	0.80
Ck1601-268	Zk1601, 268 m	Pyrite	−0.20
Ck1601-282	Zk1601, 282 m	Pyrite	−0.50
Rcy-1*		Pyrite	0.90
Rcy-2*		Chalcopyrite	−0.50
Rcy-3*		Pyrite	0.20
Rcy-4*		Chalcopyrite	0.20
Rcy-5*		Pyrite	1.20
Rcy-6*		Pyrite	0.60
Rcy-7*		Pyrite	0.70

6. Discussion and conclusions

6.1. Rock- and ore-forming ages of the Tuwu deposit

The rock- and ore-forming ages of the Tuwu copper deposit have recently been precisely constrained. Liu et al. (2003) applied the Sensitive High-mass Resolution Ion MicroProbe (SHRIMP) technique to the ore-bearing plagiogranite-porphyry. Sixteen zircons from the rock yielded a weighted mean age of 333 ± 2 Ma (95% confidence level), interpreted as the magmatic crystallization age of the plagiogranite-porphyry. Rui et al. (2002a) obtained a

Re–Os isochron age of 323 ± 2.3 Ma from molybdenite, interpreted as the early ore-forming age. In addition, Qin (2000) obtained a K–Ar age of 311.1 ± 4.6 Ma for sericites separated from two ore-bearing porphyries. These data show that the mineralization of the Tuwu deposit occurred in the period between 323 and 311 Ma, shortly after the intrusion of the ore-bearing plagiogranite-porphyry at 333 ± 2 Ma.

6.2. Geochemical characteristics of mineralized porphyries

Compared with ordinary granites, ore-bearing porphyries are characterized by a deep-seated source and shallow emplacement, and have lower initial $^{87}Sr/^{86}Sr$ ratios (Xia et al., 2002). Generally, island-arc ore-bearing porphyries have initial $^{87}Sr/^{86}Sr$ ratios in a range of 0.702 to 0.705 in accordance with derivation of ore material from the upper mantle (Titley and Beane, 1981). Initial $^{87}Sr/^{86}Sr$ ratios of porphyry-type Cu deposits in western North America range from 0.7055 to 0.7109, suggesting that crustal material may have been involved in mineralization (Titley and Beane, 1981). The initial $^{87}Sr/^{86}Sr$ ratios of the Tuwu ore-bearing plagiogranite-porphyry range from 0.7039 to 0.7067 (Rui et al., 2002a), implying an upper mantle source for the magma. However, some crustal material may have been mixed with the magma during intrusion. Sulfur isotopes in global porphyry copper deposits exhibit a narrow range, clustering close to 0‰. The $\delta^{34}S$ values of porphyry copper deposits in China are in the range of −3.5‰ to 3.0‰ (Xia et al., 2002); $\delta^{34}S$ values of the Tuwu sulfides range from −0.9‰ to +1.3‰, with a mean of 0.34‰, very close to that of meteoritic sulfur, suggesting a deep source for the sulfur in the Tuwu deposit.

Fluid inclusion homogenization temperatures typically display a wide range in most porphyry copper deposits. For example, homogenization temperatures of the Yulong Cu deposit (Tibet) are around 180 to 620 °C, salinities of ore fluids are 3% to 50% NaCl equiv., $\delta^{18}O$ values of quartz phenocrysts in ore-bearing porphyry range from +7.2‰ to +10.3‰, and fO_2 values for the mineralizing process are 10^{-15} to 10^{-35}(Rui et al., 1984). Compared with the Yulong deposit, the Tuwu deposit has relatively lower homogenization temperatures ranging from 101 to 409 °C, generally falling between 100 and 200 °C, with most values near 175 °C. Salinities in fluid inclusions range between 0.35% to 14.61% NaCl equiv., and inferred fO_2 values are 10^{-20} to 10^{-8} (Rui et al., 2001).

6.3. Adakite characteristics of the ore-bearing porphyries

In recent years, researchers have noted and documented that melts derived from a subducted slab played an important role in arc magmatism in many orogenic belts of the world (Kay, 1978; Defant and Drummond, 1990; Martin, 1999). Kay (1978) named such a rock, first identified on Adak Island, South Pacific Ocean, as adakite. Defant and Drummond (1990) summarized the geochemical characteristics of adakite as: SiO_2 >56 wt.%, Al_2O_3 >15 wt.%, 3.5 wt.%<Na_2O>7.5 wt.%, K_2O/Na_2O <0.42, low HREE (Yb <1.9 ppm) and Y (<18 ppm), high Sr (>400 ppm) and Sr/Y ratio >40, and positive Sr and Eu anomalies.

The syn-orogenic ore-bearing plagiogranite porphyries in the East Tianshan orogenic belt hosting the Tuwu deposit accord well with the above characteristics of adakites. Their SiO_2 contents range from 65.32 to 80.73 wt.% (mean 70.05 wt.%). Al_2O_3 ranges from 12.03 to 17.71 wt.%, with an average of 15.15 wt.%; K_2O/Na_2O is <1 (0.13 to 0.78) and the $Al_2O_3/(CaO+Na_2O+K_2O)$ molar ratio is >1.0 (1.05 to 1.40). They have low MgO (0.07 to 2.20 wt.%), but Mg# is moderately high, ranging from 24 to 72 (Table 1).

Trace element abundances of the Tuwu ore-bearing plagiogranite porphyries show high Sr (279 to 714 ppm); Sr/Y ratios ranging from 33.73 to 100.32 are consistent with those of adakite. Cr (6 to 17 ppm), Ni (2 to 12 ppm) and Nb (2 to 4 ppm) contents are low. In addition, Yb and Y contents are much lower than those of adakite (0.38 to 0.87 ppm, average 0.65 ppm and 4.42 to 7.90 ppm, average 5.90 ppm, respectively; Table 1), respectively, suggesting that the residual fractionation of garnet in the magma sources was much stronger than normal adakite (Qu et al., 2004).

Pearce and Cann (1973) suggested that analysis of trace elements allows the recognition of different tectonic environments for of magma generation: ocean ridge, back-arc basin ridge, volcanic-arc, collision setting, intra-plate setting and passive

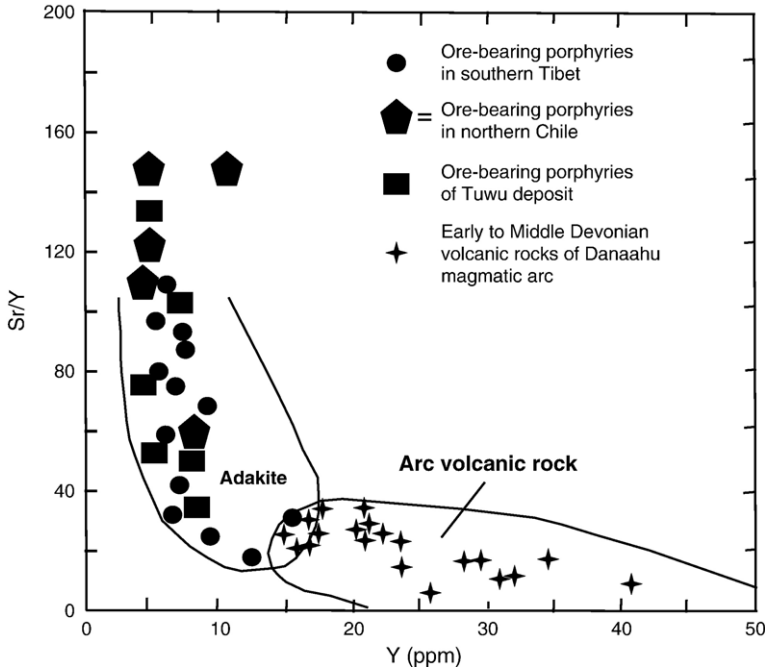

Fig. 10. Sr/Y–Y diagram (after Martin, 1999). See text for discussion.

continental margin. Brown et al. (1984) suggested that with time maturation, the volcanic arcs get richer in Rb, Th, U, Ta, Nb, Hf and Y and depleted in Ba, Sr, P, Zr and Ti. Figs. 10 and 11 show Sr/Y vs. Y and $(La/Yb)_N$ vs.$(Yb)_N$ relationships. The fields for adakites and classic volcanic arc rocks are indicated in the plots. The Tuwu ore-bearing plagiogranite porphyries fall within the adakite field, with low to moderate $(La/Yb)_N$ ratio.

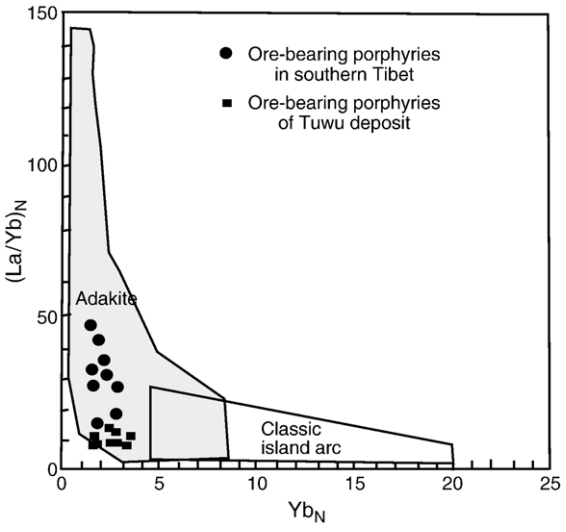

Fig. 11. $(La/Yb)_N$–$(Yb)_N$ diagram (after Martin, 1999). See text for discussion.

The Tuwu plagiogranite porphyries were formed within a tectonic framework of a volcanic arc related to interaction between the Tarim and Siberian plates during the late Paleozoic orogeny. The dominant regime was of fast convergence and thick continental crust. The geochemical signatures of adakite granitoids from the Tuwu deposit could well represent a guide for the exploration of porphyry copper deposit in the East Tianshan Mountains.

6.4. Ore-forming model for the Tuwu porphyry-copper deposit

The Chinese Eastern Tianshan is the easternmost segment of the Tianshan Mountain range in the southern Altaids, which extends eastwards through the Beishan orogenic belt to Inner Mongolia and occupies a key position between the Central Asian belts to the west and east (Xiao et al., 2004). Its geodynamic evolution is closely associated with the evolution of an ancient Tianshan Ocean between the

Tarim block and Angaran Paleozoic active margin of the Central Asia Ocean Belt (Han et al., 2003; Xiao et al., 2004). Based on the geochronological data for the tectonic and metallogenic evolution (Table 2), syn- and post-collisional Cu mineralization in the East Tianshan are recognized to belong to two distinct age groups, i.e., porphyry copper systems formed at ca. 340–320 Ma, and a variety of other deposits that formed at ca. 290–240 Ma. These are considered to be the periods of syn- and post-collisional tectonism, respectively.

The porphyry copper deposits recognized in the East Tianshan lie between the Kanguertag and Dacaotan faults. The Xinjiang Bureau of Geology and Mineral Resources (BGMR) interpreted the belt to represent a Carboniferous island arc. However, Rui et al. (2002a) and Qin (2000) reported Rb–Sr isochron and single-grain zircon U–Pb data from host rock of the Tuwu copper deposit indicating an age range of 356 to 369 Ma, which suggests that they formed in the late Devonian, and not in the Early Carboniferous. The Devonian Dananhu and Tousuquan Formations mainly consist of calc-alkaline felsic volcanic lavas and tuffs; the Carboniferous Xiaorequanzi and Dikaner Formations is mainly composed of lavas, pyroclastic rocks, greywacke and carbonates (Xiao et al., 2004). The Devonian–Carboniferous tholeiitic basalt and calc-alkaline andesite suite were interpreted to be volcanic rocks belonging to an island arc (Yang et al., 2000; Zhou et al., 2001). Rocks of the arc are intruded by a number of batholiths comprising diorite, granodiorite, and granite bodies (Mao et al., 2005). SHRIMP zircon U–Pb ages of 383 ± 9 Ma for arc monzonitic granite, and 357.3 ± 6.2 Ma for a granodiorite from these intrusions (Song et al., 2002). The grano-porphyry related magmas at the Tuwu–Yandong were emplaced ranging from 333 ± 2 Ma to 334 ± 2 Ma (Liu et al., 2003). These data indicate that the arc has a Middle-Devonian to Early Carboniferous age (Xiao et al., 2004). Qin (2000) and Rui et al. (2002a) obtained single grain zircon ages of 356 ± 8 Ma and 361 ± 8 Ma, respectively, for granite of the Tuwu–Yandong copper mine. A Re–Os isochron date of 322.7 ± 2.3 Ma of ores from Tuwu–Yandong deposits (Rui et al., 2002a), and a $^{39}Ar/^{40}Ar$ age of 347 ± 2 Ma of sericite for altered grano-porphyry from Yandong mine (Qin, 2000). These data indicate that magmatism and associated porphyry copper mineralization lasted until the end of the Early Carboniferous. The Dananhu–Tousuquan arc formed as a result of the northward subduction of the Tianshan Ocean.

In Fig. 12, we present a tectonic model consistent with the regional observations outlined above, and taking account of porphyry copper systems and intrusions in the Dananhu arc of the East Tianshan orogenic belt. In our model, the Tuwu complex developed in a period of north-dipping subduction within the evolution of the southern Dananhu arc, and has the essential characteristics of adakites. In

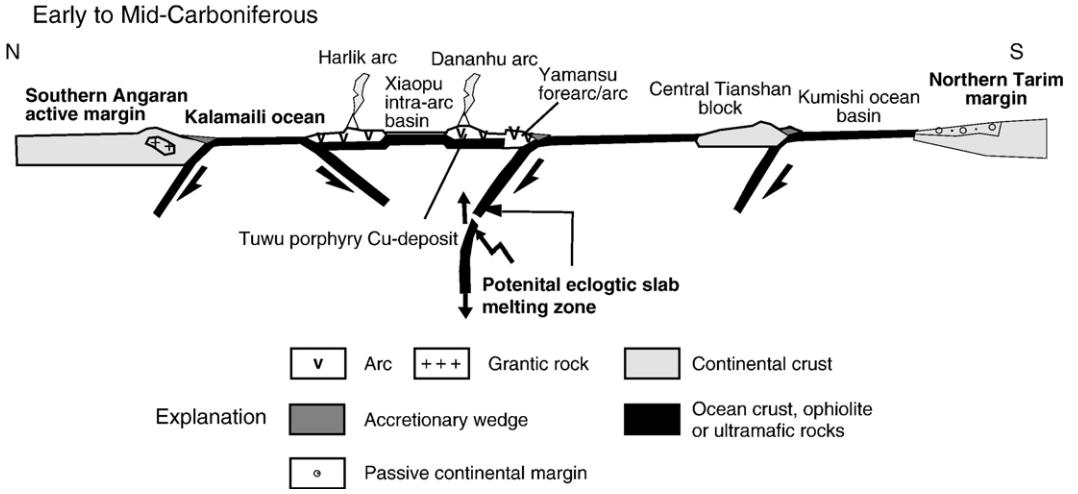

Fig. 12. Schematic diagrams showing the late Paleozoic evolution and formation of Tuwu porphyry Cu deposit and other metal deposits in the Eastern Tianshan (after Xiao et al., 2004); see text for discussion.

the Early to Mid-Carboniferous, a northward-dipping oceanic slab generated a magmatic arc in the south of Dananhu area. At the leading edge on the upper plate, the Tuwu complex was first to experience adakitic magmatism in response to the melting of thermally anomalous slab material. Slab consumption may have continued by shallow subduction between adakite magmatism and arc collision. Opening a slab window beneath the Tuwu complex could lead to multiple pulses of magmatism and production of crustal melts (Thorkelson and Taylor, 1989; Percival et al., 2003). In light of the high transition metal contents of the Tuwu suite, elevated Cu contents are possible in these intrusive rocks. Such a hypothesis of the slab melting model can be more efficient in recycling the hydrothermal Cu-sulfides of the downgoing oceanic slab (Qu et al., 2004).

Acknowledgements

This paper was initially presented at the workshop of IGCP 473 in Urumuqi, China, in August, 2003. We are grateful to R.J. Goldfarb for constructive discussions and review on an early version of the manuscript, and to W.S. Chen for assistance in the fluid inclusion study. Thanks are also given to K.Z. Qin, Z.C. Zhang, Y.T. Wang, J.Y. Li, T.L. Ma, and L.C. Zhang for thoughtful discussions and providing relevant references. This study was financially supported by a national project of China (2001CB409801), a CAS Knowledge Innovation Project (KZCX3-SW-119-01) and NSFC (40172080).

References

Allen, M.B., Windley, B.F., Zhang, C., 1992. Paleozoic collisional tectonics and magmatism of the Chinese Tianshan, Central Asia. Tectonophysics 220, 89–115.

Briqueu, L., Bougault, H., Joron, J.L., 1984. Quantification of Nb, Ta, Ti and V anomalies in magmas associated with subduction zones—petrogenetic implications. Earth and Planetary Science Letters 68, 297–308.

Brown, G.C., Thorpe, R.S., Webb, P.C., 1984. The geochemical characteristics of granitoids in contrasting arcs and comments on magma source. Journal of the Geological Society (London) 141, 411–426.

Chen, W.M., Qu, X.M., 2002. Host rocks of Tuwu–Yandong (Porphyry) copper deposit in Tianshan Mountains. Mineral Deposits 21 (4), 331–340 (in Chinese with English abstract).

Coleman, R.G., 1989. Continental growth of Northwest China. Tectonics 8, 621–635.

Defant, M.J., Drummond, M.S., 1990. Derivation of some modern magmas by melting of young subducted lithosphere. Nature 347, 662–665.

Gao, J., Li, M.S., Xiao, X.C., Tang, Y.Q., He, G.Q., 1998. Palaeozoic tectonic evolution of the Tianshan orogen, northwestern China. Tectonophysics 287, 213–231.

Gu, X.X., Tang, J.X., Wang, C.S., Chen, J.P., He, B.B., 2003. Himalayan magmatism and porphyry copper–molybdenum mineralization in the Yulong ore belt, East Tibet. Mineralogy and Petrology 78, 1–20.

Han, C.M., 2002. Research on Metallogenic Series of Copper Deposits in East Tianshan Mountains. China University of Geosciences, Beijing. 138 pp. (in Chinese with English abstract).

Han, C.M., Zhao, G.C., 2003. Major types and characteristics of the late Paleozoic ore deposits, East Tianshan, Northwest China. International Geology Review 45, 798–814.

Han, C.M., Rui, Z.Y., Mao, J.W., Yang, J.M., Wang, Z.L., Yuan, W.M., 2003. Geological characteristics of the Tuwu copper deposit, Hami, Xinjiang. In: Mao, J.W., Goldfarb, R.J., Seltmann, R., Wang, D.H., Xiao, W.J., Hart, C. (Eds.), Tectonic Evolution and Metallogeny of the Chinese Altay and Tianshan Proceeding Volume of the International Symposium of the IGCP-473 Project in Urumqi, IAGOD Guidebook Series, pp. 249–260.

He, G.Q., Li, M.S., Liu, D.Q., 1994. Palaeozoic Crustal Evolution and Mineralization in Xinjiang of China. Xinjiang People's Publishing House, Urimqi. 245 pp. (in Chinese with English abstract).

Kay, R.W., 1978. Aleutian magnesian andesites: melts from subducted Pacific Ocean crust. Journal of Volcanology and Geothermal Research 4, 117–132.

Lan, C.Y., Jahn, B.M., Mertzman, S.A., Wu, T.W., 1996. Subduction-related granitic rocks of Taiwan. Journal Southeast Asian Earth Science 14, 11–28.

Li, W.M., Ren, B.C., Yang, X.K., Li, Y.Z., Chen, Q., 2002. The intermediate-acid intrusive magmatism and its geodynamic significance in Eastern Tianshan region. Northwest Geology 35, 41–64 (in Chinese with English abstract).

Liu, D.Q., Tang, Y.L., Zhou, R.H., 2001. Metallogenic conditions and prospecting and prospecting. Xinjiang Geology 19, 43–48 (in Chinese with English abstract).

Liu, D.Q., Chen, Y.C., Wang, D.H., 2003. A discussion on problems related to mineralization of Tuwu–Yandong Cu–Mo ore field in Hami, Xinjiang. Mineral Deposits 22, 334–344 (in Chinese with English abstract).

Luchitskaya, M.V., Morozov, O.L., Palandzhyan, S.A., 2005. Plagiogranite magmatism in the Mesozoic island-arc structure of the Pekulney Ridge, Chukotka Peninsula, NE Russia. Lithos 79, 251–269.

Ma, R.S., Shu, L.S., Sun, J.Q., 1997. Tectonic Framework and Crust Evolution of Eastern Tianshan Mountains. Geological Publishing House, Beijing. 202 pp. (in Chinese with English abstract).

Mao, J.W., Yang, J.M., Qu, W.J., 2002. Re–Os dating of Cu-Ni sulfide ores from Huangshandong deposit in Xinjiang and its geological significance. Mineral Deposits 21, 330–339 (in Chinese with English abstract).

Mao, J.W., Yang, J.M., Qu, W.J., 2003. Re–Os age of Cu–Ni ores from the Huangshandong Cu–Ni sulfide deposit in the East Tianshan Mountains and its implication for geodynamic processes. Acta Geologica Sinica 77, 220–226.

Mao, J.W, Goldfarb, R.J., Wang, Y.T., Hart, C.J.R., Wang, Z.L., Yang, J.M., 2005. Late Paleozoic base and precious metal deposits, East Tianshan, Xinjiang, China: characteristics and geodynamic setting. Episodes 28, 1–14.

Martin, H., 1999. Adakite magma: modern analogues of Archean granitoids. Lithos 46, 411–429.

Pearce, J.A., Cann, J.R., 1973. Tectonic setting of volcanic rocks determined using trace element analysis. Earth and Planetary Science Letters 19, 290–300.

Percival, J.A., Stern, A.A., Rayner, N., 2003. Archean adakite from the Ashunipi complex, eastern Superior Province, Canada: geochemistry, geochronology and tectonic significance. Contributions to Mineralogy and Petrology 145, 265–280.

Qin, K.Z., 2000. Metallogenesis in relation to central-Asia style orogeny of northern Xinjiang. Institute of Geology and Geophysics, Chinese Academy of Sciences, Beijing 230 pp. (in Chinese with English abstract).

Qin, K.Z., Fang, T.H., Wang, S.L., Wang, X.D., 2001. Discovery of the Kalatage Cu–Au mineralized district and its prospecting potentiality, Paleozoic Window (uplift) at the south margin of the Tu-Ha basin. Chinese Geology 28 (3), 16–23 (in Chinese with English abstract).

Qin, K.Z., Sun, S., Li, J.L., 2002. Paleozoic epithermal Au and porphyry Cu deposits in North Xinjiang, China: Epochs, features, tectonic linkage and exploration significance. Resource Geology 52, 291–300.

Qin, K.Z., Zhang, L.C., Xiao, W.J., Xu, X.W., Yan, Z., Mao, J.W., 2003. Overview of major Au, Cu, Ni and Fe deposits and metallogenic evolution of the Eastern Tianshan Mountains, Northwestern China. In: Mao, J.W., Goldfarb, R.J., Seltmann, R., Wang, D.H., Xiao, W.J., Hart, C. (Eds.), Tectonic Evolution and Metallogeny of the Chinese Altay and Tianshan: Proceedings Volume of the International Symposium of the IGCP-473 project in Urumqi, IAGOD Guidebook Series, pp. 227–248.

Qu, X.M., Hou, Z.Q., Li, Y.G., 2004. Melt components derived from a subducted slab in late orogenic ore-bearing porphyries in the Gangdese copper belt, Southern Tibetan plateau. Lithos 74, 131–148.

Rollinson, H.R., 1993. Using Geochemical Data: Evaluation, Presentation, Interpretation. Longman Scientific and Technical, Singapore. 352 pp.

Rui, Z.Y., Huang, Z.K., Qi, G.M., 1984. Porphyry copper (molybdenum) deposits in China. Geological Publishing House, Beijing. 350 pp. (in Chinese with English abstract).

Rui, Z.Y., Wang, F.T., Li, H.H., 2001. Advance of the porphyry copper belt of the East Tianshan Mountains, Xinjiang. Chinese Geology 28 (2), 11–16 (in Chinese with English abstract).

Rui, Z.Y., Wang, L.S., Wang, Y.T., Liu, Y.L., 2002a. Discussion on metallogenic epoch of Tuwu and Yandong porphyry copper deposits in East Tianshan Mountains, Xinjiang. Mineral Deposits 21 (1), 16–22 (in Chinese with English abstract).

Rui, Z.Y., Liu, Y.L., Wang, L.S., Wang, Y.T., 2002b. The eastern Tianshan porphyry belt in Xinjiang and its tectonic framework. Acta Geologica Sinica 76 (1), 83–94. (in Chinese with English abstract).

Şengör, A.M.C., Natal'in, B.A., Burtman, V.S., 1993. Evolution of the Altaid tectonic collage and Palaeozoic crustal growth in Eurasia. Nature 364, 299–307.

Şengör, A.M.C., Natal'in, B.A., Burtman, V.S., 1996. Turkic-type orogeny and its role in the making of the continental crust. Annual Review of Earth and Planetary Science 24, 263–337.

Song, B., Li, J.Y., Li, W.Q., Wang, K.Z., Wang, Y., 2002. SHRIMP dating of zircon from Dananhu and Keziekalasai granitoid batholith in southern margin of Tuiha basin, East Tishan, NW China and their geological implication. Xinjiang Geology 20, 342–345 (in Chinese with English abstract).

Titley, S.R., Beane, R.E., 1981. Porphyry copper deposits: Part 1. Geological settings, petrology, and tectogenesis, and Part 2. Hydrothermal alternation and mineralization. Economic Geology, 214–269 (75th Anniversary Volume).

Thorkelson, D.J., Taylor, R.P., 1989. Cordillera slab window. Geology 17, 833–836.

Wang, F.T., Feng, J., Hu, J.W., 2001. Characteristics and significance of the Tuwu porphyry copper deposit, Xinjiang. Chinese Geology 28, 36–39 (in Chinese with English abstract).

Windley, B.F., Allen, M.B., Zhang, C., 1990. Palaeozoic accretion and Cenozoic redeformation of the Chinese Tianshan range, Central Asia. Geology 18, 128–131.

Wood, D.A., Joron, J.L., Treuil, M., 1979. A reappraisal of the use trace elements to classify and discriminate between magma series erupted in different tectonic settings. Earth and Planetary Science Letters 68, 297–308.

Xia, B., Chen, G., Wang, H., 2002. Analysis on the tectonic background of superlarge porphyry copper deposits in the world. Science in China (Series D) 32, 87–95 (in Chinese).

Xia, L.Q., Xu, X.Y., Xia, Z.C., Li, X.M., Ma, Z.P., Wang, L.S., 2004. Petrogenesis of Carboniferous rift-related volcanic rocks in the Tianshan, northwestern China. Geological Society of America Bulletin 116, 419–433.

Xiao, X.C., Tang, Y.Q., Feng, Y.M., Zhu, B.Q., Li, J.Y., Zhao, M., 1990. On the tectonic evolution of the northern Xinjiang, Northwest China. Geoscience of Xinjiang 1, 47–68 (in Chinese with English abstract).

Xiao, W.J., Zhang, L.C., Qin, K.Z., Sun, S., Li, J.L., 2004. Paleozoic accretionary and collisional tectonics of the Eastern Tianshan (China): implications for the continental growth of central Asia. American Journal of Science 304, 370–395.

Yang, X.K., 1996. Basic features of the plate tectonics in eastern Tianshan. Xinjiang Geology 14, 221–227 (in Chinese with English abstract).

Yang, X.K., Ji, J.S., Luo, G.C., Tao, H.X., 1997. Plate tectonics and metal mineralization in Eastern Tianshan. Journal of Xi'an College of Geology 19, 34–42 (in Chinese with English abstract).

Yang, X.K., Zhang, L.C., Ji, J.S., Zeng, Z.R., Tao, H.X., 1998. Deformation characters of the Qiugemingtashi–Huangshan duc-

tile shear zone in eastern Tianshan. Journal of Xi'an Engineering University 20, 11–18 (in Chinese with English abstract).

Yang, X.K., Cheng, H.B., Ji, J.S., Luo, G.C., Tao, H.X., 2000. Analysis on gold and copper ore-forming setting with ore-forming system of Eastern Tianshan. Journal of Xi'an Engineering University 22, 7–14. (in Chinese with English abstract).

Zhang, L.C., Xiao, W.J., Qin, K.Z., Ji, J.S., Yang, X.K., 2004a. Types, geological features and geodynamic significances of gold–copper deposits in the Kanggurtag metallogenic belt, eastern Tianshan, NW China. International Journal of Earth Sciences 93, 224–240.

Zhang, L.C., Qin, K.Z., Ying, J.F., Xia, B., Shu, J.S., 2004b. The relationship between ore-forming processes and adakitic rock in Tuwu–Yandong porphyry copper metallogenic belt, eastern Tianshan mountains. Acta Petrologica Sinica 20 (2), 259–268.

Zhou, J.Y., Cui, B.F., Xiao, H.L., Chen, S.Z., Zhu, D.M., 2001. The Kangguertag–Huangshan collision zone of bilateral subduction and its metallogenic model and prognosis in Xinjiang, China. Volcanology and Mineral Resources 22, 252–263 (in Chinese with English abstract).

Zhou, M.F., Lesher, C.M., Yang, Z.X., Li, J.W., Sun, M., 2004. Geochemistry and petrogenesis of 270 Ma Ni–Cu–(PGE) sulfide-bearing mafic intrusions in the Huangshan district, Eastern Xinjiang, Northwest China: implications for the tectonic evolution of the Central Asian orogenic belt. Chemical Geology 209, 233–257.